88 KSME International Journal, Vol. 11, No. 1, pp. 88~95, 1997

Idle Speed Modeling and Optimal Control of a Spark-Ignition Engine

Shin Hyuk Joo* and Kwang Min Chun**

(Received April 22, 1996)

A model of engine dynamics is developed. The model is a MISO (Multi Input Single Output) linear model which has two inputs and one output. One input is the spark timing, and the other is the ISCV (Idle Speed Control Valve) position. The output is the angular speed of an engine. The reliability of the developed model is confirmed by comparing the measured response of the engine to step inputs and external disturbance with the simulation results. In order to reduce the steady state error, an integrator state is inserted to the state equation. An engine idle speed controller is designed using optimal control theory based on the model. The performance variation of the controller to the various design parameters is simulated. On the basis of the simulation and the experimental data, the design parameters are determined. The developed controller reduced the idle speed drop caused by an external load change and recovered the desired idle speed in one second.

Key Words: Idle, Idle Speed, Spark Timing, ISCV, MISO Linear Model, Optimum Control

1. Introduction

Idle speed control is becoming more important as automobile engines in a city are being operated often at idle condition due to the bad traffic congestion. A large number of studies about the engine modeling and the idle speed control has been carried out and many publications (Cassidy, 1980 ; Morris, 1983 ; Hendricks, 1986, 1990, 1991a, 1991b ; Onder, 1993 ; Kjergaard, 1994) were presented recently. Hendricks developed a nonlinear mean value engine model (Hendricks, 1990) and Kjergaard presented an advanced nonlinear engine idle speed control systems. (Kjergaard, 1994) In this study, two nonlinear control strategies were compared with conventional PID and LQR(Linear Quadratic Regulator) designs. But the nonlinear mean value engine model is very complicated and there is little advantage to the simple linear models. Onder presented model-based multivariable speed and A/F ratio control of a SI engine. (Onder, 1993) Most of the studies about the idle speed control focus on the engine speed variations caused by the engine load changes.

There are two kinds of engine load changes. One is the rapid external changes, and the other is the slowly varying changes in operating conditions or engine condition. Rapid external load changes are caused by the accessories such as the air conditioning, steering pump drive, etc. Slowly varying changes in operating conditions or engine condition are changes in the ambient pressure and temperature, fuel quality, and lubricant temperature, etc. In this study, only the rapid external load changes are considered.

Drivers don't like the idle speed variation caused by the engine load changes. In order to decrease the idle speed variation, the conventional engine control systems use the P or PI regulators. Such regulators are fairly easy to be tuned. But

* Dept. of Mechenical Engineering, Yonsei University, Shinchon-Dong 134, Seodaemoon-Gu, Seoul, Korea.

** Depet. of Mechenical Engineering, Yonsei University, Shinchon-Dong 134, Seodaemoon-Gu, Seoul, Korea.

such regulators cannot be designed with a very high loop gain. For this reason, conventional engine control systems commonly use the feedforward to help the regulators maintain the idle speed at the desired level. But for a number of reasons, this is undesirable. The most important reason is that the external loads applied to an engine may be changed in time and more power consuming equipment can be installed in a vehicle after it left the factory. In this study, the feedforward is not used and the controller is designed using the optimum control theory (Kim, J.S, 1994)

If external load is applied abruptly, idle speed will drop rapidly. To maintain the idle speed constant, the engine torque must be increased by increasing the intake air and the amount of fuel injected or by advancing the ignition time. As idle speed control variables, the ignition time and the ISCV (Idle Speed Control Valve) are used, and the latter changes the air flow rate. In order to develop an idle speed control system, a modeling of engine dynamics is carried out and confirmed by comparison with the experiments. Based on this model, a controller is designed using the optimum control theory.

2. Apparatus

The experimental equipment is composed of an engine, a dynamometer, an air flow meter, a spark timing controller (Yang Byung-Yul, 1994; Kim Jong-Jin, 1994), an ISCV, rotational speed sensor, etc. The spark timing controller is developed using PPI-8253 counter and IBM-PC. Fig. 1 is the schematic diagram of experimental equipment.

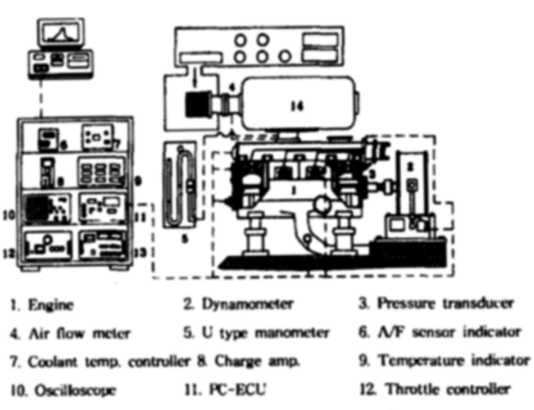

Fig. 1 Schematic deagram of experimental equipment

3. Engine Modeling

In order to develop an idle speed control system, a model for the engine dynamics is needed. In our study a linear model is developed for the simplicity. Figure 2 is the flow chart of the developed engine model.

3.1 The theory of engine modeling

3.1.1 Dynamics of ISCV control motor

Although the dynamics of the ISCV are nonlinear due to limitations of friction and inertia effect, we used a linear model for the simplicity.

$$\frac{dS}{dt}=K_1(S_{commd.}-S) \tag{1}$$

where K_1: A constant which is determined by modeling experiment

S: ISCV Position

$S_{commd.}$: Input command of ISCV Position

3.1.2 Dynamics of intake manifold

The state equation of the ideal gas is Eq.(2)

$$P_m V_m = m_m R T_m \tag{2}$$

where, P_m: Intake manifold pressure

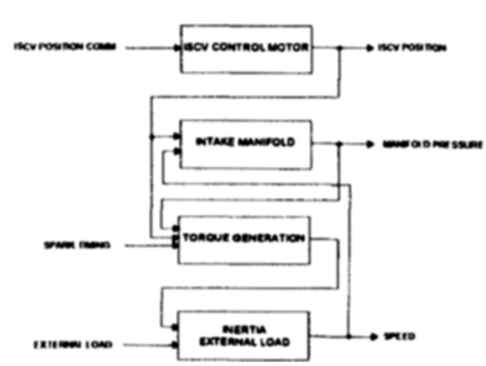

Fig. 2 Flow chart of an engine model

V_m: Intake manifold volume
m_m: Mass of the air in the Intake manifold
T_m: Temperature of the air in the Intake manifold
R: Gas constant

Differentiating the Eq. (2) yields

$$\frac{dP_m}{dt}V_m + P_m\frac{dV_m}{dt} = \frac{dm_m}{dt}RT_m + m_mR\frac{dT_m}{dt} \quad (3)$$

The manifold volume and the air temperature can be assumed to be constant. Equation (3) is simplified to Eq. (4)

$$\frac{dP_m}{dt} = \frac{RT_m}{V_m}\frac{dm_m}{dt} \quad (4)$$

the rate of manifold mass change is

$$\frac{dm_m}{dt} = \dot{m}_{m,i} - \dot{m}_{m,o} \quad (5)$$

where, $\dot{m}_{m,i}$: Air flow rate into the manifold
$\dot{m}_{m,o}$: Air flow rate into the manifold

$\dot{m}_{m,i}$ is a function of manifold pressure and ISCV position, and $\dot{m}_{m,o}$ is a ffunction o manifold pressure and engine speed.

$$\dot{m}_{m,i} = f_1(P_m, S) \quad (6)$$

$$\dot{m}_{m,o} = f_2(P_m, n) \quad (7)$$

Linearization of Eqs. (6) and (7) yields

$$\Delta\,\dot{m}_{m,i} = K_3\Delta P_m + K_4\Delta S \quad (8)$$

where, K_3, K_4: Constants which are determined by modeling experiment

$$\Delta\,\dot{m}_{m,o} = K_5\Delta P_m + K_6\Delta n \quad (9)$$

where, K_5, K_6: Constants which are determined by modeling experiment

At the steady state condition, $\dot{m}_{m,i}$ equals $\dot{m}_{m,o}$. The modeling parameters K_3, K_4, K_5, K_6 can be found by the experiments which measure the air flow rate for various P_m, n, S at steady state condition. From the Eqs. (4), (5), (8) and (9) the final model for the intake manifold is deduced as Eq. (10)

$$\frac{dP_m}{dt} = K_2K_4\Delta S + K_2(K_3 - K_5)\Delta P_m - K_2K_6\Delta n \quad (10)$$

where, $K_2 = \frac{RT_m}{V_m}$

3.1.3 Dynamics of engine torque, inertia, external load

There are many parameters which affect the engine torque. The angular speed of engine, intake manifold pressure, spark timing, A/F ratio, coolant temperature and intake air temperature, etc can change the engine torque. In this study, we considered only the engine speed, intake manifold pressure and spark timing, which are the most important variables. The experiments for modeling were carried out with all parameters fixed except the engine speed, intake pressure and spark timing constant. So, we can express the engine torque as a function of engine speed, intake pressure, and spark timing. Equation (11) is a linearized model of the engine torque.

$$\Delta T_{engine} = K_7\Delta n + K_8\Delta P_m + K_9\Delta\alpha_{ign} \quad (11)$$

where, K_7, K_8, K_9: Constants which are determined by modeling experiment

Torque is a function of polar moment of inertia and angular acceleration as Eq. (12).

$$T = J\dot{\omega} \quad (12)$$

By converting the unit and considering the external load in Eq. (12), we can derive Eq. (13)

$$\dot{n} = K_{10}(T_{engine} - T_{load}) \quad (13)$$

where, $K_{10} = \frac{1}{J}\frac{2\pi}{60}$

The linearization of Eq. (13) yields Eq. (14)

$$\Delta\dot{n} = K_{10}(T_{engine} - T_{load}) \quad (14)$$

Using Eqs. (11) and Eq. (14) we finally developed a equation for the angular acceleration as a function of angular speed, manifold pressure, ignition time, and external load.

$$\Delta\dot{n} = K_{10}(K_7\Delta n + K_8\Delta P_m + K_9\Delta\alpha_{ign.} - \Delta T_{load}) \quad (15)$$

Equation (15) is a linearized model of engine torque, inertia and external load.

3.1.4. The final engine model

From Eqs. (1), (10) and (15) we can derive Eq (16) which is the final engine model as matrix form.

$$\begin{bmatrix}\Delta\dot{S}\\ \Delta\dot{P}_m\\ \Delta\dot{n}\end{bmatrix}=\begin{bmatrix}-K_1 & 0 & 0\\ K_2K_4 & K_2(K_3-K_5) & -K_2K_6\\ 0 & K_{10}K_8 & K_{10}K_7\end{bmatrix}\begin{bmatrix}\Delta S\\ \Delta P_m\\ \Delta n\end{bmatrix}+\begin{bmatrix}K_1 & 0 & 0\\ 0 & 0 & 0\\ 0 & K_{10}K_9 & -K_{10}\end{bmatrix}\begin{bmatrix}\Delta S_{comn.}\\ \Delta \alpha_{ign}\\ \Delta T_{load}\end{bmatrix} \quad (16)$$

3.2 Experiments for engine modeling

3.2.1 ISCV control motor

The value of K1 was determined by measuring the time spent to move ISCV 10000, 20000 and 30000 steps.

3.2.2 Intake manifold

When engine operates at constant ISCV position, the intake manifold pressure can be changed by applying the external load. Figure 3 is the result of the experiment which measured the intake air flow rate. In each line, ISCV position is kept constant and manifold pressure is changed by applying different external loads. The intake air flow rate is measured when engine operates at steady state. In Fig. 3, the average of the slopes is the K_3. The value of K_4 can be found from graphs with the ISCV Position as x axis in the same way.

When engine operates at constant speed, the intake manifold pressure can be changed by changing the ISCV position. Figure 4 is the result of the experiment which measured the intake air flow rate. In each line, engine speed is kept constant and manifold pressure is changed by moving the ISCV. In Fig. 4 the average of the slopes is the K_5. The value of K_6 can be found from graphs with the engine speed as horizontal axis in the same way.

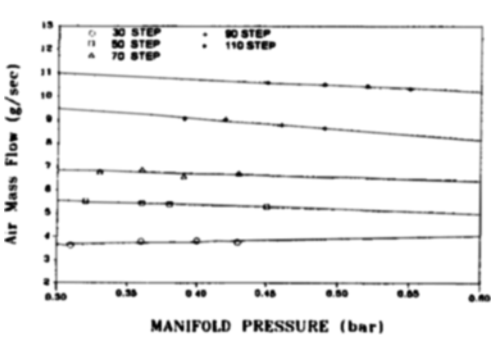

Fig. 3 Air mass flow versus manifold pressurem at 30, 50, 70, 90, 110 step ISCV position

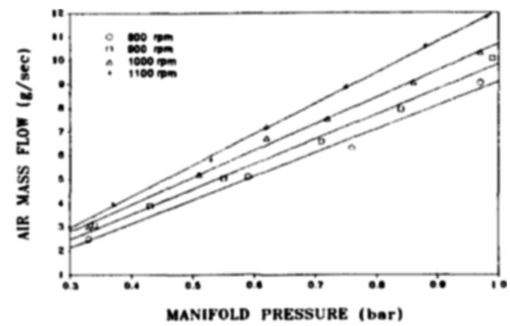

Fig. 4 Air mass flow versus manifold pressure at 800, 900, 1000, 1100 rpm

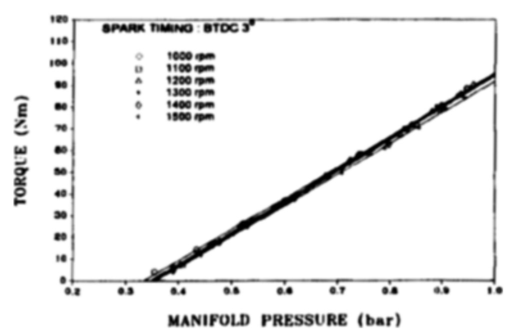

Fig. 5 Torque versus manifold pressure at 1000, 1100, 1200, 1300, 1400, 1500 rpm, S/T: BTDC 30

3.2.3 Engine torque

In order to develop a model of engine torque, we measured the changes of engine torque for the change of intake manifold pressure at engine speeds of 1000, 1100, 1200, 1300, 1400 and 1500 rpm, changing the ignition timing from 3 to 19 by 2 crank angle degrees. Figure 5 is one of the results of experiments for developing a engine torque model. It can be seen that the engine torque varies linearly with the pressure change of the intake manifold. The results of other spark timings are very similar to that in Fig. 5. From the spark timing changing experiment results, we determined the K_8 in Eq. (8). The average of the slopes of all lines is K_8. Similar to K_4 and K_6, the value of K_9 can be determined from the graphs with the spark timing as horizontal axis and the value of K_7 from the graphs with the engine speed

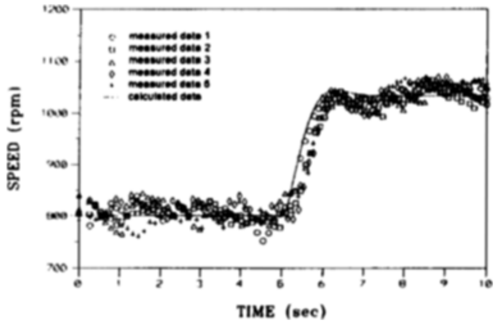

Fig. 6 Measured and calculated engine speed responses corresponding to the 10 step ISCV position open

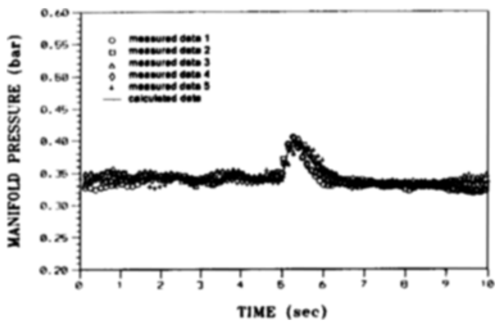

Fig. 7 Measured and calculated manifold pressure responses corresponding to the 10 step ISCV position open

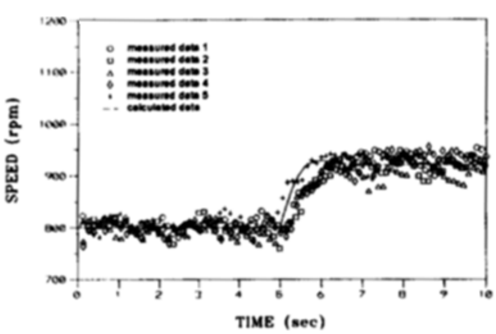

Fig. 8 Measured and calculated engine speed responses corresponding to the 10 degrees spark timing advance

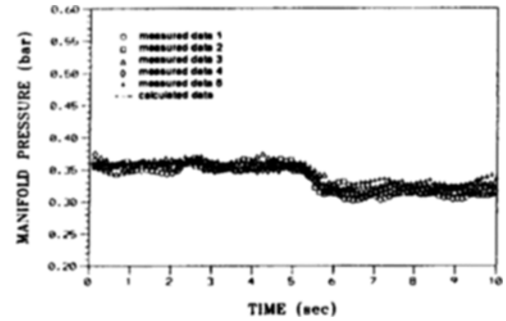

Fig. 9 Measured and calculated manifold pressure responses corresponding to the 10 degrees spark timing advance

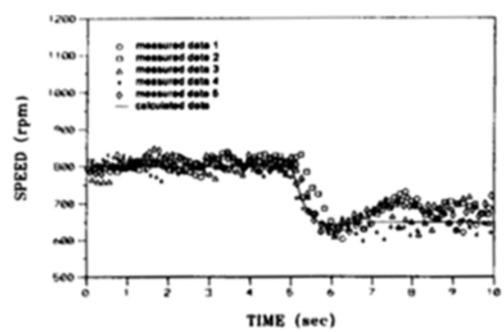

Fig. 10 Measured and calculated engine speed responses corresponding to the external load

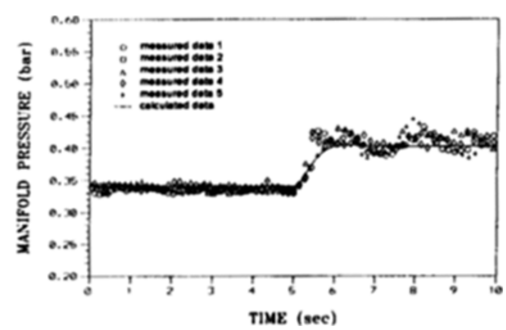

Fig. 11 Measured and calculated manifold pressure responses corresponding to the external load

as horizontal axis.

3.3 Model confirmation

Modeling an engine is to predict the engine response to various input changes. To test the accuracy of the model, the experimental data is compared with the calculated results. During experiments, the changes of the engine state variables to the various step inputs were taken.

Figures 6 and 7 show that the developed model predicts well the changes of the engine speed and intake manifold pressure corresponding to the step input of ISCV 10 steps open. Each solid line is the calculated result and the dot lines are the experimental data. In Fig. 8, Fig. 9, Figs. 10, and

Fig. 11 it can be seen that the model developed predicts well the changes of the engine speed and manifold pressure also for different load changes. The step input is 10 degrees spark timing advance in Figs.8, Fig.9 and 6 Nm external load in Fig.10 and Fig.11.

4. Idle Speed Control

4.1 The composition of the idle speed control system

Figure 12 is the block diagram of the idle speed control system. The engine speed and manifold pressure are supplied to the controller as an input and the controller determines the ISCV position S_{commd}, and the spark timing $\alpha_{ign.}$ as outputs. In response to the S_{commd}, the ISCV control motor moves forward or backward and changes the air flow rate. In response to the $\alpha_{ign.}$, the spark generator changes the spark timing.

4.2 Design of an idle speed controller

When the engine is operated at steady state condition, there should not be any steady state error. In order to eliminate the steady state error, we included an integral term to the state equation. A common method of introducing integration action into a system described by a set of state equations is to augment the system equations with the integral of the variable of interest. Equation (17) is derived in this way where ni is the time integral of the Δn.

$$\begin{bmatrix} \Delta \dot{S} \\ \Delta \dot{P}_m \\ \Delta \dot{n} \\ \dot{n}_i \end{bmatrix} = \begin{bmatrix} -K_1 & 0 & 0 & 0 \\ K_2K_4 & K_2(K_3-K_5) & -K_2K_6 & 0 \\ 0 & K_{10}K_8 & K_{10}K_7 & 0 \\ 0 & 0 & 1 & 0 \end{bmatrix} \begin{bmatrix} \Delta S \\ \Delta P_m \\ \Delta n \\ n_i \end{bmatrix} + \begin{bmatrix} K_1 & 0 \\ 0 & 0 \\ 0 & K_{10}K_9 \\ 0 & 0 \end{bmatrix} \begin{bmatrix} \Delta S_{commd.} \\ \Delta \alpha_{ign.} \end{bmatrix} + \begin{bmatrix} 0 \\ 0 \\ -K_D \\ 0 \end{bmatrix} \Delta T_{load} \quad (17)$$

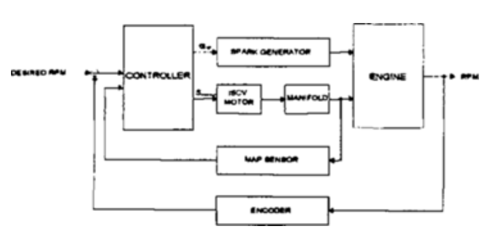

Fig. 12 Block diagram of the idle speed control system

In controller design we used the standard optimum control theory. In this case, the state variables (Δn, ΔP_m, n_i) and the input terms ($\Delta S_{commd.}$, $\Delta \alpha_{ign.}$) should be minimized. Therefore the quadratic cost criteria can be expressed as Eq. (18).

$$J = \lim_{t_1 \to \infty} \int_{t_0}^{t_1} [\zeta_1(\Delta_n)^2 + \zeta_2(\Delta P_m)^2 + \zeta_3(n_i)^2 + \rho_1(\Delta S_{commd.})^2 + \rho_2(\Delta \alpha_{ign.})^2] \quad (18)$$

ζ_1, ζ_2, ζ_3, ρ_1, and ρ_2 are the weighting constants, and should be determined by experiments or simulations. The total amount of the quadratic cost criteria should be minimized. Therefore the increase of the ρ results in the decrease of the input terms. If the input terms are to be increased, ρ should be decreased. Similarly, if the effects of Δn, ΔP_m, Δn_i are to be increased, ζ_1, ζ_2, ζ_3 should be decreased respectively. Once we determine these weighting constants, the input terms which minimize the quadratic cost criteria J can be determined by solving the Riccati's equation.

In order to determine the design parameters, control simulations were performed. Figure 13 is the result of the simulation about the controller performance for various design parameters such as ζ and ρ. It is assumed that 6 Nm of the external load is applied to the engine at 0 second. In Fig. 13, Simul. 1 is the result of simulation which predicts the engine speed change when the external load is applied to the engine. A controller which has design parameters ζ and ρ is installed to the engine. Simul. 2 is the result of the simulation about the controller performance with same ζ value but larger ρ value. The larger ρ of Simul. 2 results in the decrease of the input terms. Therefore, the engine speed drops more and it takes longer time to recover the speed in Simul. 2. In Simul. 3, the same design parameters were used as Simul. 1 with lower ζ_3. The decrease of ζ_3 results in the increase of the effect of ni. Many other simulations were performed to find the effect of the varying design parameters. On the

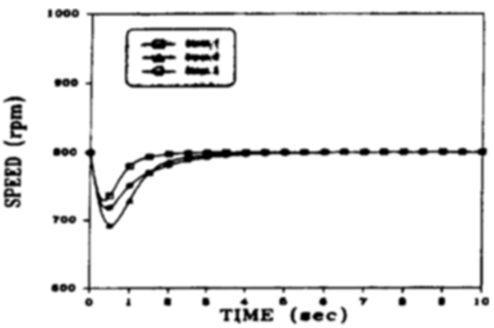

Fig. 13 Results o the idle speed control simulation

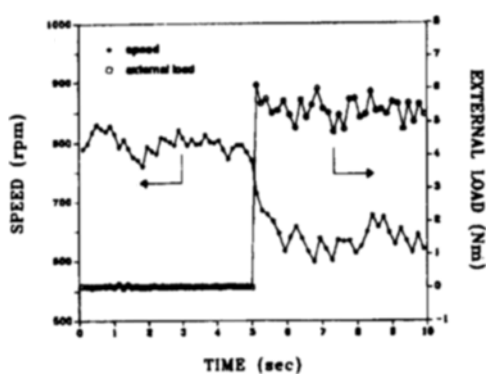

Fig. 14 External load and reponse of the engine speed without a controller

basis of these simulation results, the idle speed control experiments were carried out, and the optimum design parameters ζ_1, ζ_2, ζ_3, ρ_1 and ρ_2 were finally determined.

4.3 Result of the idle speed control experiment

The idle speed control experiment is carried out by measuring the variations of engine speed. The external load of 6 Nm is applied abruptly when the engine is operating at 800 rpm. Figure 14, and Fig. 15 are the results of these experiments. In Fig. 14, when the controller is not installed to the engine, the external load of 6 Nm decreased as the idle speed decreased from 800 rpm to 600 rpm. In Fig. 15, when a controller is installed, the idle speed drop is less han 70 rpm, and the idle speed is recovered to 800 rpm within 1 second.

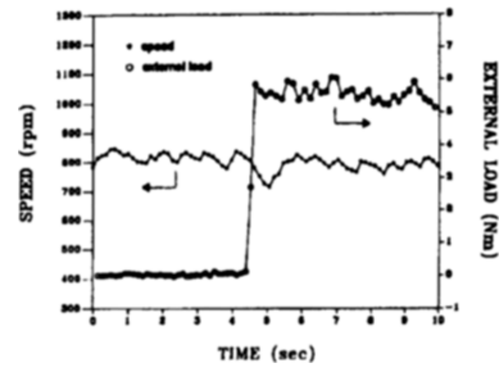

Fig. 15 External load and response of the engine speed with a optimal controller

5. Conclusion

In this study, an engine model at idle speed has been developed which is composed of ISCV control motor, intake manifold pressure, and engine torque. An optimum engine idle speed controller has also been developed.

Conclusion of this study are as follow.

(1) The experimentally developed linear engine model predicts the engine responses well to such step inputs as ISCV open, spark timing advance, and external load.

(2) 6 Nm external load change decreased the idle speed from 800 rpm to 600 rpm without a controller. With the optimum idle speed controller developed in this study, the idle speed drop decreased from 200 rpm to 70 rpm, and the speed recovered to 800 rpm in 1 second.

Reference

Cassidy, J. F., Athens, M. and Lee, W. H., 1980, "On the Design of Electronic Automotive Engine Controls Using Linear Quadratic Control Theory," *IEEE Trans. on Automotive Control,* Vol. AC-25, No. 5.

Hendricks, E., and Poulsen, N., 1986, "Minimum Energy Control of Large Diesel Engines," *SAE Technical Paper* No. 861191,

Hendricks, E. and Sorenson, S. C., "Mean Value Modelling of Spark Ignition Engines," *SAE Paper* 900616

Hendricks, E. and Sorenson, S. C, "SI Engine Controls and Mean Value Engine Modelling," *SAE Paper* 910258

Hendricks, E., 1991, Transient Errors in Classical SI Engine Controllers, *American Control Conference* (1991 ACC), Paper No. TP-14, 15:00,

Heywood, J. B., 1988, *Internal Combustion Engine Fundamentals*, McGraw Hill,

Kjergaard, L., Nielsen, S., Vesterholm, T. and Hendricks, E., "Advanced Nonlinear Engine Idle Speed Control Systems," *SAE Paper* 940974

Kim Jong-Jin, 1994, "A Study of Knock Control Using the Cylinder Block Vibration Signal," *Dept. of Mech. Engineering The Graduate School Yonsei University,*

Kim, J. S, 1994, "Linear Control System," Chung-Mun-Gak,

Morris, R. L. and Powell, B. K., 1983, "Mordern Control Applications in Idle Speed Control," Paper, No. WA4-11:45, *American Control Conference* (*ACC*).

Onder, C. H., Geering, H. P., "Model-Based Multivariable Speed and Air-to-Fuel Ratio Control of an SI Engine," *SAE Paper* 930859

Yang Byung-Yul, 1994, "Basic Study of Idle Speed Control in a Spark-Ignition Engine," *Dept. of Mech. Engineering The Graduate School Yonsei University,*